ALBERTA-THY-12-15, DESY-15-100, SFB/CPP-14-127, TTP15-021, TUM-HEP-1001/15

Next-to-next-to-next-to-leading order QCD prediction for the top anti-top S-wave pair production cross section near threshold in e^+e^- annihilation

Martin Beneke,[1] Yuichiro Kiyo,[2] Peter Marquard,[3] Alexander Penin,[4, 5] Jan Piclum,[6] and Matthias Steinhauser[5]

[1] *Physik Department T31, James-Franck-Straße 1, Technische Universität München, D-85748 Garching, Germany*
[2] *Department of Physics, Juntendo University, Inzai, Chiba 270-1695, Japan*
[3] *Deutsches Elektronen Synchrotron DESY, Platanenallee 6, D-15738 Zeuthen, Germany*
[4] *Department of Physics, University of Alberta, Edmonton AB T6G 2J1, Canada*
[5] *Institut für Theoretische Teilchenphysik, Karlsruhe Institute of Technology (KIT), 76128 Karlsruhe, Germany*
[6] *Albert Einstein Center for Fundamental Physics, Institute for Theoretical Physics, Sidlerstrasse 5, CH-3012 Bern, Switzerland*

(Dated: June 17, 2015)

We present the third-order QCD prediction for the production of top-anti-top quark pairs in electron-positron collisions close to the threshold in the dominant S-wave state. We observe a significant reduction of the theoretical uncertainty and discuss the sensitivity to the top quark mass and width.

PACS numbers: 14.65.Ha, 12.38.Bx, 13.66.Bc

Among the main motivations for building a future high-energy electron-positron collider in steps of increasing center-of-mass energy are precise measurements at $\sqrt{s} \approx 345\,\text{GeV}$ close to the production threshold of top anti-top quark pairs. The peculiar behaviour of the cross section allows for the precise determination of a number of Standard Model parameters, most prominently the top quark mass. To date the most precise measurement of $m_t = 173.34 \pm 0.27(\text{stat}) \pm 0.71(\text{syst})\,\text{GeV}$ comes from the hadron colliders Fermilab Tevatron and CERN LHC [1] and is based on the reconstruction of the top and anti-top quarks through their decay products. This approach and the value quoted above are plagued by unknown relations of the extracted mass value m_t to top quark masses in the pole or $\overline{\text{MS}}$ renormalization scheme, which may well exceed 1 GeV. At hadron colliders there are also methods to determine directly a well-defined top quark mass, such as the extraction of m_t from top quark cross section measurements. However, the final precision is of the order of a few GeV and thus significantly worse. At an electron-positron collider, on the other hand, scans of the top anti-top pair production threshold can lead to very precise measurements of well-defined mass values with a statistical accuracy of only 20-30 MeV [2, 3]. Besides the top quark mass also its decay width and the strong coupling constant can be extracted with an accuracy of 21 MeV [3] and 0.0009 [2], respectively. A recent study has shown that for a Higgs boson with a mass of about 125 GeV the top quark Yukawa coupling can be obtained with a statistical uncertainty of only 4.2% [3]. These numbers pose several challenges to theory.

A crucial input to reach the aimed precision is a precise calculation of the top anti-top pair production cross section in the threshold region. While the fundamental theory of quantum chromodyanmics (QCD) is well-established, performing calculations of quantum corrections to the very high accuracies demanded here is very difficult indeed. The problem is further complicated by the fact that in the threshold region the colour Coulomb potential $\propto \alpha_s/r$, where α_s denotes the strong coupling, can no longer be treated as a perturbation even though $\alpha_s \ll 1$. Standard perturbation theory in α_s breaks down and resummation is required.

The relevant techniques have been developed in the 1990s in the framework of effective field theory (EFT), which accounts for the different dynamical scales in the problem. For a heavy quark anti-quark system at threshold there are three relevant scales, the hard scale m, the potential and soft scale mv, and the ultrasoft scale mv^2, where m denotes the mass of the quark and v its velocity. Since $v \ll 1$ there is indeed a strong hierarchy between these scales and thus it is possible to construct a tower of effective theories taking QCD as starting point. In a first step one arrives at non-relativistic QCD (NRQCD) [4, 5] by integrating out the hard modes. Afterwards all other modes are integrated out except the ones which are needed to describe a physical non-relativistic quark anti-quark system—potential modes for the quarks with energy $\mathcal{O}(mv^2)$ and three-momentum $\mathcal{O}(mv)$, and ultrasoft gluons with four-momentum $\mathcal{O}(mv^2)$. The corresponding theory is potential NRQCD (PNRQCD) [6]. In practice, the separation of the different modes and scales is done with the threshold expansion of Feynman diagrams [7]. The concepts and tools required to perform the computation of the cross section near threshold with the accuracy reported in this Letter are summarized in [8].

Within the EFT the normalized total cross section can be written in the form (see, e.g., [8])

$$
\begin{aligned}
R &= \frac{\sigma(e^+e^- \to t\bar{t} + X)}{\sigma_0} \qquad (1)\\
&= \frac{18\pi}{m_t^2}\,\mathrm{Im}\left\{ c_v \left[c_v - \frac{E}{m_t}\left(c_v + \frac{d_v}{3} \right) \right] G(E) + \ldots \right\},
\end{aligned}
$$

where c_v and d_v denote NRQCD matching coefficients, $E = \sqrt{s} - 2m_t$, $G(E)$ is the non-relativistic two-point Green function, and $\sigma_0 = 4\pi\alpha^2/(3s)$ is the cross section for the production of a $\mu^+\mu^-$ pair in the limit of large center-of-mass energy $\sqrt{s}$. The ellipsis refers to terms which are beyond the next-to-next-to-next-to-leading order ($\mathrm{N^3LO}$) in the expansion in α_s and v.

The next-to-next-to-leading order (NNLO) QCD corrections were computed in the late 1990s [9–14], and the results of several groups were summarized and compared in [15]. The first NNLO calculations were expressed in terms of the top quark pole mass and found large corrections to the location of the cross section peak near threshold casting doubt on the possibility to perform a very accurate mass measurement. It was pointed out in [16] that these corrections are an artifact of the renormalization convention, which could be avoided by choosing a scheme that is less sensitive to uncalculable long-distance effects of QCD. Subsequent calculations of the top antitop threshold all employ mass renormalization conventions different from the on-shell scheme. Here we use the potential-subtracted (PS) mass [17]. However, even with this improvement, large corrections to the height of the cross section peak are observed at NNLO, which motivates the $\mathrm{N^3LO}$ QCD calculation, the result of which is reported in this Letter.

There has been quite some effort to resum logarithmic terms in the velocity of the produced top quarks and obtain so-called next-to-next-to-leading logarithmic (NNLL) approximations [18, 19]. The most complete analysis has been performed in [20], where new ultrasoft terms have been included. The NNLL approximation already contains the $\ln v$ enhanced terms of the $\mathrm{N^3LO}$ correction, but not the "constant" terms. Partial results have shown that these constant terms are as large as the logarithmic terms, at least in individual pieces of the calculation [21–23].

Since more than ten years several groups have computed building blocks of the $\mathrm{N^3LO}$ correction, which can be subdivided into matching coefficients of NRQCD and PNRQCD and higher order corrections to $G(E)$. In [8] a detailed discussion of the individual contributions can be found. Among them are the three-loop corrections to the static potential [24–26], certain $\mathcal{O}(\epsilon)$ terms of higher-order potentials in dimensional regularization [8, 27, 28], and three-loop fermionic corrections to c_v [29, 30]. Furthermore, ultrasoft corrections to $G(E)$ [21] and all Coulombic contributions up to the third order [31]. Recently, the last two building blocks have been computed, which allows us to put together for the first time a prediction for the cross section near threshold with $\mathrm{N^3LO}$ accuracy. First, the purely gluonic three-loop correction to the QCD-to-NRQCD vector current matching coefficient c_v appearing in

$$\bar{t}\gamma^i t = c_v\, \psi^\dagger\sigma^i\chi + \frac{d_v}{6m_t^2}\,\psi^\dagger\sigma^i\,\mathbf{D^2}\chi + \ldots, \qquad (2)$$

has been computed [22], completing the matching calculations up to the so-called singlet diagrams. (In other contexts and at second order [32] these singlet contributions have been shown to be small.) Second, the calculation of the PNRQCD two-point function $G(E)$ of currents $\psi^\dagger\sigma^i\chi$ has been completed to third order in PNRQCD perturbation theory with the computation of the single and double non-Coulomb potential insertions [23]. We note that PNRQCD includes the leading-order Coulomb potential in the unperturbed Lagrangian. Perturbation theory around this interacting Lagrangian amounts to the resummation of the standard loop expansion in α_s. The various contributions have been encoded in a `Mathematica` program.

There is a number of non-QCD effects, which are expected to be relevant to a realistic cross section prediction. a) The existence of a Higgs boson affects the production process and generates an additional short-range potential. b) The same holds for electroweak and electromagnetic corrections, amongst which is the electrostatic potential between the charged top quarks. c) The rapid electroweak decay $t \to W^+ b$ of the top quark is responsible for the fact that the distinct toponium bound-state poles are smeared to a broad resonance near threshold (see Fig. 1 below). For the same reason, it will be mandatory to consider the process $e^+e^- \to W^+W^-b\bar{b}$ including the non-resonant contributions. Non-resonant effects have been computed to NLO and partially to NNLO accuracy [33–36], and can be naturally separated in the framework of unstable particle EFT [37, 38]. d) Electromagnetic initial-state radiation generates large logarithms $\ln(4m_t^2/m_e^2)$, where m_e is the electron mass, which must be summed. e) Furthermore, there are collider-specific effects such as beamstrahlung and the luminosity spectrum [2]. Neither of these effects is discussed further in the following. The purpose of the present Letter is to demonstrate that the third-order QCD calculation brings the QCD contributions under control, which is a prerequisite for all further studies, including the non-QCD effects above. We refer to [39] for a study of the Higgs contribution and the prospects for determining the Yukawa coupling, and the impact of the NLO non-resonant correction on the top mass determination.

We now turn to the discussion of the $\mathrm{N^3LO}$ QCD result. In order to better compare the successive orders we do not include here the known contribution [40] from the axial-vector Z-boson coupling in the production process $e^+e^- \to Z^* \to t\bar{t}$, which starts at NNLO and is below 1%. Our result therefore refers to the S-wave production cross section. Unless stated otherwise we use the following input values for the top quark mass in the PS scheme, the top quark width and the strong coupling constant:

$$m_t^{\rm PS}(\mu_f = 20\,\mathrm{GeV}) = 171.5\ \mathrm{GeV},\ \Gamma_t = 1.33\ \mathrm{GeV},$$
$$\alpha_s(M_Z) = 0.1185 \pm 0.0006\,. \qquad (3)$$

Furthermore, the renormalization scale is varied between 50 and 350 GeV. Note that an unstable behaviour of the perturbative series is expected for scales below $\mu \approx$ 40 GeV [23, 31]. The scale μ_w related to the separation of resonant and non-resonant contributions to the $e^+e^- \to W^+W^-b\bar{b}$ process is fixed to $\mu_w = 350\,\mathrm{GeV}$. The dependence on this choice is numerically negligible.

The main result of this Letter is shown in Fig. 1, where

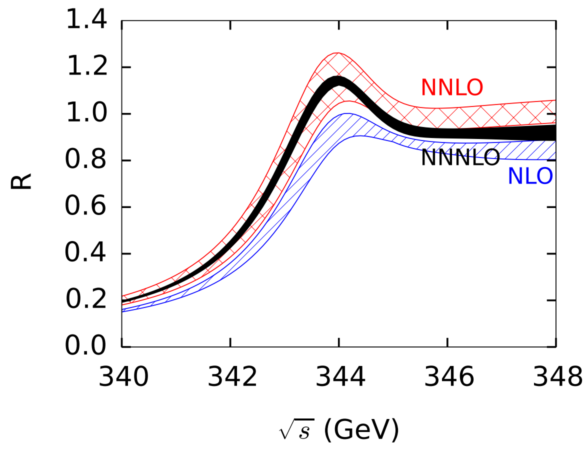

FIG. 1. Scale dependence of the cross section near threshold. The NLO, NNLO and N^{3}LO result is shown in blue, red and black, respectively. The renormalization scale is varied between 50 and 350 GeV.

the total cross section is shown as a function of the center-of-mass energy $\sqrt{s}$. The previous NLO and NNLO predictions are also shown for comparison to the new N^{3}LO result (black, solid). The bands are obtained by variation of the renormalization scale in the specified range. After the inclusion of the third-order corrections one observes a dramatic stabilization of the perturbative prediction, in particular in and below the peak region. In fact, the N^{3}LO curve is entirely contained within the NNLO one. This is different above the peak position where a clear negative correction is observed when going from NNLO to N^{3}LO. For example, 3 GeV above the peak this amounts to -8%. This arises from the large negative three-loop correction to the matching coefficient c_v [22].

The theoretical precision of the third-order QCD result as measured by the residual scale dependence is highlighted in Fig. 2, which shows $R(\mu)$ normalized to a reference prediction defined at $\mu = 80\,\mathrm{GeV}$. The width of the shaded band corresponds to an uncertainty of about $\pm 3\%$ with some dependence on the center-of-mass energy $\sqrt{s}$. The figure also shows the sensitivity to the top-quark width. The two solid lines refer to the cross section with Γ_t changed by $\pm 100\,\mathrm{MeV}$ to 1.43 and 1.23 GeV, respectively, computed with $\mu = 80\,\mathrm{GeV}$ and normalized to the reference prediction. Decreasing the width implies a sharper peak, i.e. an enhancement in the peak region, and a suppression towards the non-resonant region below the peak. A few GeV above the peak the cross section is largely insensitive to the width. Increasing the width leads to the opposite effects. This pattern is clearly seen in Fig. 2, which also demonstrates that a $\pm 100\,\mathrm{MeV}$ deviation from the width predicted in the Standard Model leads to a cross section change near and below the peak far larger than the uncertainty from scale variation.

We now turn to the question to what accuracy the top quark mass can be determined. Even if we focus only on the theoretical accuracy, a rigorous analysis requires accounting for the specifics of the energy points of the threshold scan and the correlations. However, a good indication is already provided by looking at the position and height of the resonance peak. Fig. 3 shows this information at LO, NLO, NNLO and N^{3}LO, where the outer error bar reflects the uncertainty due to the renormalization scale and α_s variation, added in quadrature, and the inner error bar only takes the α_s uncertainty into account. The central point refers to the value at the reference scale $\mu = 80\,\mathrm{GeV}$. There is a relatively big jump from LO to NLO of about 310 MeV, approximately 150 MeV from NLO to NNLO, which reduces to only 64 MeV from NNLO to N^{3}LO. Furthermore, the NNLO and N^{3}LO uncertainty bars show a significant overlap.

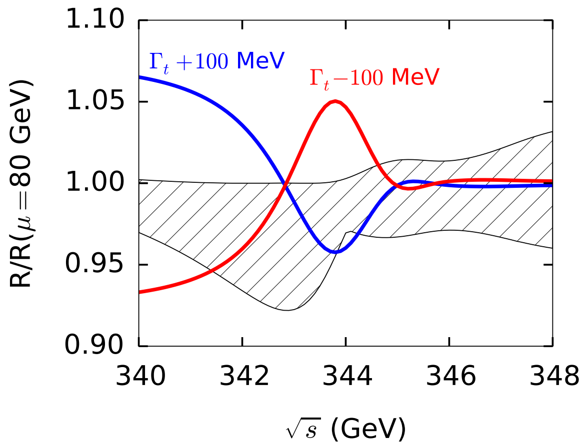

FIG. 2. Scale dependence (hatched area) of the N^{3}LO cross section relative to the reference prediction. Overlaid are predictions for two different values of Γ_t, again normalized to the reference prediction. See text for details.

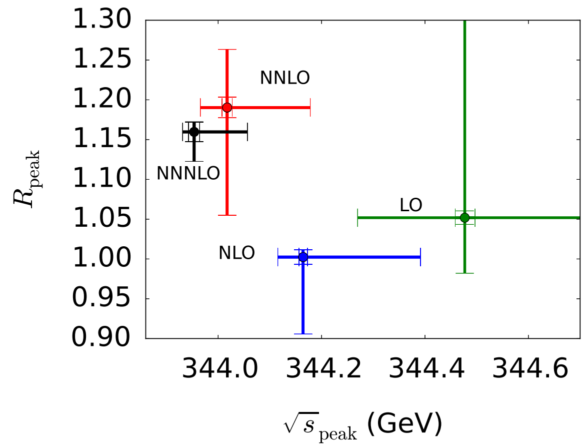

FIG. 3. Position and height of the cross section peak at LO, NLO, NNLO and N^{3}LO. The unbounded range of the LO error bars to the right and up are due to the fact that the peak disappears for large values of the renormalization scale.

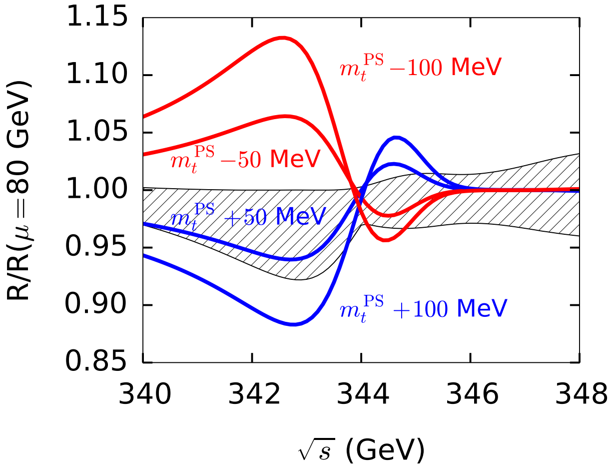

FIG. 4. Relative cross section variation when the top quark mass is changed by ± 50 and ± 100 MeV, superimposed on the scale dependence of the N^{3}LO cross section prediction. See text for details.

Taking into account only the uncertainty from scale variation the uncertainty of the peak position amounts to ± 60 MeV at N^{3}LO with a factor two improvement relative to NNLO. The improvement is even larger for the peak height, which is relevant to the top quark width and Yukawa coupling determination as discussed above and in [39]. Note that these conclusions refer to the top quark PS mass (and not the pole mass), and correspondingly to the $\overline{\mathrm{MS}}$ mass, which can be related to the PS mass with an accuracy of about 20 MeV [41].

We display the sensitivity of the cross section to the top quark mass in Fig. 4, which is the same as Fig. 2, except that the curves superimposed to the relative scale variation of the N^{3}LO cross section now refer to shifts of the top PS mass by ± 50 and ± 100 MeV. The shape of these curves is easily understood, as a change of the mass by δm_t mainly shifts the peak of the cross section and is largely equivalent to a shift of $\sqrt{s}$ by $2\delta m_t$. The figure demonstrates that the largest sensitivity to the mass occurs around 1.5 GeV below the peak. A variation of the mass by ± 50 MeV changes the cross section at $\sqrt{s} = 342.5$ GeV by $\pm 6\%$, compared to a scale uncertainty of $\pm 3.8\%$. Accounting for the characteristic shape of variation, we may conclude that the theoretical uncertainty on the top quark mass should be well below ± 50 MeV.

Comparing the N^{3}LO result to the NNLO results with $\ln v$ resummation [19, 20], we notice that in both approaches the correction to the peak height relative to NNLO is negative (with the default scale choice) [19], while the theoretical uncertainty of the cross section normalization is reduced to about $\pm 3\%$ compared to the $\pm 5\%$ quoted in [20].

In summary, we presented the third-order QCD calculation of the top quark production cross section in e^+e^- annihilation in the threshold region. Despite the extra complication of non-relativistic resummation to all orders in QCD perturbation theory, this is one of only a few collider processes now known at N^{3}LO in QCD. The third-order calculation leads to a large reduction of the QCD theoretical uncertainty to about $\pm 3\%$, and thereby solves a long-standing issue regarding the reliability of the QCD prediction for this process. Top quark mass determinations with theoretical errors below 50 MeV now appear feasible. Further improvement by going to the next order in QCD is currently unrealistic. However, it would be desirable to include the information about logarithmic effects in v beyond N^{3}LO already contained in the NNLL computations [19, 20]. More importantly, with QCD effects under control as demonstrated here, further studies of non-QCD effects are now well motivated—and required.

ACKNOWLEDGMENTS

This work has been supported by DFG Sonderforschungsbereich Transregio 9 "Computergestützte Theoretische Teilchenphysik", and the DFG Gottfried Wilhelm Leibniz programme. The work of Y.K. was supported in part by Grant-in-Aid for Scientific Research No. 26400255 from MEXT, Japan. P.M. was supported in part by the European Commission through contract PITN-GA-2012-316704 (HIGGSTOOLS). The work of A.P. is partially supported by NSERC.

[1] ATLAS and CDF and CMS and D0 Collaborations, arXiv:1403.4427 [hep-ex].
[2] K. Seidel, F. Simon, M. Tesar and S. Poss, Eur. Phys. J. C **73**, 2530 (2013), arXiv:1303.3758 [hep-ex].
[3] T. Horiguchi, A. Ishikawa, T. Suehara, K. Fujii, Y. Sumino, Y. Kiyo and H. Yamamoto, arXiv:1310.0563 [hep-ex].
[4] B. A. Thacker and G. P. Lepage, Phys. Rev. D **43** (1991) 196.
[5] G. P. Lepage, L. Magnea, C. Nakhleh, U. Magnea and K. Hornbostel, Phys. Rev. D **46** (1992) 4052 [hep-lat/9205007].
[6] A. Pineda and J. Soto, Nucl. Phys. Proc. Suppl. **64**, 428 (1998) [hep-ph/9707481].
[7] M. Beneke and V. A. Smirnov, Nucl. Phys. B **522**, 321 (1998) [hep-ph/9711391].
[8] M. Beneke, Y. Kiyo and K. Schuller, arXiv:1312.4791 [hep-ph].
[9] A. H. Hoang and T. Teubner, Phys. Rev. D **58**, 114023 (1998) [hep-ph/9801397].
[10] K. Melnikov and A. Yelkhovsky, Nucl. Phys. B **528**, 59 (1998) [hep-ph/9802379].

[11] A. A. Penin and A. A. Pivovarov, Nucl. Phys. B **550**, 375 (1999) [hep-ph/9810496].

[12] M. Beneke, A. Signer and V. A. Smirnov, Phys. Lett. B **454**, 137 (1999) [hep-ph/9903260].

[13] A. H. Hoang and T. Teubner, Phys. Rev. D **60**, 114027 (1999) [hep-ph/9904468].

[14] T. Nagano, A. Ota and Y. Sumino, Phys. Rev. D **60**, 114014 (1999) [hep-ph/9903498].

[15] A. H. Hoang, M. Beneke, K. Melnikov, T. Nagano, A. Ota, A. A. Penin, A. A. Pivovarov and A. Signer *et al.*, Eur. Phys. J. direct C **2**, 1 (2000) [hep-ph/0001286].

[16] M. Beneke, in: Proceedings of the 33rd Rencontres de Moriond: Electroweak Interactions and Unified Theories, Les Arcs, France, 14-21 Mar 1998, hep-ph/9806429.

[17] M. Beneke, Phys. Lett. B **434**, 115 (1998) [hep-ph/9804241].

[18] A. H. Hoang, A. V. Manohar, I. W. Stewart and T. Teubner, Phys. Rev. D **65**, 014014 (2002) [hep-ph/0107144].

[19] A. Pineda and A. Signer, Nucl. Phys. B **762**, 67 (2007) [hep-ph/0607239].

[20] A. H. Hoang and M. Stahlhofen, JHEP **1405** (2014) 121, arXiv:1309.6323 [hep-ph].

[21] M. Beneke and Y. Kiyo, Phys. Lett. B **668** (2008) 143, arXiv:0804.4004 [hep-ph].

[22] P. Marquard, J. H. Piclum, D. Seidel and M. Steinhauser, Phys. Rev. D **89** (2014) 3, 034027, arXiv:1401.3004 [hep-ph].

[23] M. Beneke, Y. Kiyo and K. Schuller, "Third-order correction to top-quark pair production near threshold II. Potential contributions", to be published.

[24] A. V. Smirnov, V. A. Smirnov and M. Steinhauser, Phys. Lett. B **668**, 293 (2008), arXiv:0809.1927 [hep-ph].

[25] A. V. Smirnov, V. A. Smirnov and M. Steinhauser, Phys. Rev. Lett. **104**, 112002 (2010), arXiv:0911.4742 [hep-ph].

[26] C. Anzai, Y. Kiyo and Y. Sumino, Phys. Rev. Lett. **104**, 112003 (2010), arXiv:0911.4335 [hep-ph].

[27] S. Wüster, Heavy quark potential at order α_s^2/m^2 [in German], Diploma Thesis RWTH Aachen University (2003).

[28] M. Beneke, Y. Kiyo, P. Marquard, A. Penin, J. Piclum, D. Seidel and M. Steinhauser, Phys. Rev. Lett. **112** (2014) 15, 151801, arXiv:1401.3005 [hep-ph].

[29] P. Marquard, J. H. Piclum, D. Seidel and M. Steinhauser, Phys. Lett. B **678**, 269 (2009), arXiv:0904.0920 [hep-ph].

[30] P. Marquard, J. H. Piclum, D. Seidel and M. Steinhauser, Nucl. Phys. B **758**, 144 (2006) [hep-ph/0607168].

[31] M. Beneke, Y. Kiyo and K. Schuller, Nucl. Phys. B **714**, 67 (2005) [hep-ph/0501289].

[32] B. A. Kniehl, A. Onishchenko, J. H. Piclum and M. Steinhauser, Phys. Lett. B **638**, 209 (2006) [hep-ph/0604072].

[33] M. Beneke, B. Jantzen and P. Ruiz-Femenia, Nucl. Phys. B **840**, 186 (2010), arXiv:1004.2188 [hep-ph].

[34] A. A. Penin and J. H. Piclum, JHEP **1201** (2012) 034, arXiv:1110.1970 [hep-ph].

[35] B. Jantzen and P. Ruiz-Femenia, Phys. Rev. D **88**, 054011 (2013), arXiv:1307.4337 [hep-ph].

[36] P. Ruiz-Femenia, Phys. Rev. D **89** (2014) 9, 097501, arXiv:1402.1123 [hep-ph].

[37] M. Beneke, A. P. Chapovsky, A. Signer and G. Zanderighi, Phys. Rev. Lett. **93** (2004) 011602 [hep-ph/0312331].

[38] M. Beneke, A. P. Chapovsky, A. Signer and G. Zanderighi, Nucl. Phys. B **686** (2004) 205 [hep-ph/0401002].

[39] M. Beneke, A. Maier, J. Piclum and T. Rauh, to be published.

[40] M. Beneke, J. Piclum and T. Rauh, Nucl. Phys. B **880** (2014) 414, arXiv:1312.4792 [hep-ph].

[41] P. Marquard, A. V. Smirnov, V. A. Smirnov and M. Steinhauser, Phys. Rev. Lett. **114** (2015) 14, 142002, arXiv:1502.01030 [hep-ph].